Available online at www.sciencedirect.com
ScienceDirect
Trans. Nonferrous Met. Soc. China 31(2021) 2949−2961
Transactions of Nonferrous Metals Society of China
www.tnmsc.cn

Characterization of mechanical and corrosion properties of cryorolled Al 1100 alloy: Effect of annealing and solution treatment

S. A. ZAKARIA[1], A. S. ANASYIDA[1], H. ZUHAILAWATI[1], B. K. DHINDAW[2], N. A. JABIT[1], A. ISMAIL[3]

1. Structural Materials Niche Area, School of Materials & Mineral Resources Engineering, Universiti Sains Malaysia, 14300 Nibong Tebal, Penang, Malaysia;
2. Indian Institute of Technology Kharagpur 721302, India;
3. Department of Materials Engineering and Design Faculty of Mechanical and Manufacturing Engineering, Universiti Tun Hussein Onn Malaysia, 86400 Batu Pahat, Johor, Malaysia

Received 5 October 2020; accepted 11 May 2021

Abstract: Effect of annealing and solution treatment prior to cryorolling on the formation of initial structure influencing microstructure formation from nano to micron scale and resultant mechanical and corrosion properties in Al 1100 alloy has been studied in detail. Before subjecting to 50% cryorolling, samples were pre-annealed at 250 °C for 2 h and pre-solution treated at 540 °C for 1 h. X-ray diffraction and HRTEM techniques were used to understand the crystallite size, lattice strain and dislocation configuration in the processed alloy. The results indicate that the pre-annealed sample has the highest grain aspect ratio (4.43), the smallest crystallite size (37.53 nm), the highest lattice strain (9.12×10^{-3}) and the highest dislocation density (45.16×10^{13} m^{-2}) among the tested sample. The pre-annealed sample shows a significant improvement of 43.44%, 24.64% and 20.33% in hardness, ultimate tensile strength and yield strength. Both pre-annealed and pre-solution treated samples show improved corrosion resistance when compared to cryorolled samples without any pre-treatment, with the pre-annealed sample showing the best corrosion resistance.
Key words: cryorolling; Al 1100 alloy; pre-heat treatment; nanostructure; ultrafine-grain; mechanical properties; corrosion resistance

1 Introduction

Deformation at cryogenic temperature has emerged as a potential method to develop ultrafine-grained (UFG) materials in aluminium alloy with improved mechanical properties [1]. Cryorolling has been well established as one of the potential techniques for producing ultrafine-grained sheets of pure metal and alloys from its bulk counterpart by deforming them at cryogenic temperatures with much less strain compared to other severe plastic deformation (SPD) processes performed at ambient/high temperature [2−4]. The process was first investigated by WANG et al [5] in which they rolled Cu at liquid nitrogen temperature to 93% thickness reduction and the yield strength was found to have increased by almost six times. The high strength was attributed to the high density of dislocations formed due to its sub-zero processing which effectively suppressed the dynamic recovery [6]. Due to the enhanced properties offered by ultrafine grains, most of the research has been well developed in variety of approaches, such as in structural characterization, microhardness and tensile properties. However, less effort has been made to research the effect of initial microstructure by pre-heat treatment on the formation of ultrafine grains in aluminum alloys. Pre-heat treatment is essential to ensure that the

Corresponding author: A. S. ANASYIDA, Tel: +604-5995216, E-mail: anasyida@usm.my
DOI: 10.1016/S1003-6326(21)65705-9

initial microstructure formed enhances the formation of ultrafine grains during cryorolling.

Several researchers have investigated the effects of pre-heat treatment prior to the cryorolling process. RAO et al [7] have reported the effect of pre-annealing on microstructure and mechanical properties of Al 6061 alloy while KRISHNA et al [8] and PANIGRAHI and JAYAGANTHAN [9] have investigated the effects of various solution heat treatment temperature on the mechanical properties of the alloy. They have found that the strength was improved significantly with an increase in solution heat treatment temperature. Another study by SEKHAR et al [10] on Al 5052 alloy showed that pre-annealing at 300 °C for 90 min has improved the mechanical properties of the cryorolled (CR) alloy. The tensile strength and yield strength were claimed to have improved by nearly 76.8% and 59.6%, respectively, after imparting 50% thickness reduction. GASHTI et al [11] annealed AA1050 at 370 °C for 7200 s to homogenize the microstructure and relieve the residual stresses present in the sheet material prior to accumulative roll bonding (ARB) process. After 9 cycles of ARB, the YS and UTS increased approximately to 160 MPa and 192 MPa, respectively, which showed about three and two times higher values than those of the annealed sample. This is an indication of efficient strengthening of the material during ARB process. Meanwhile, SIVAPRASAD et al [12] applied solution treatment on commercial pure aluminium at 540 °C for 1 h and quenched in water prior to cryorolling. Comparison of annealing and solution treatment prior to cryorolling which are important aspects for initial structure formation that enhance the development of ultrafine grains in aluminium alloy has less been studied in detail. In view of this scenario, and with the aim of providing new insights into the influence of the initial structure on the properties of cryorolled aluminium alloy, this work was therefore carried out to characterize the mechanical and corrosion properties of cryorolled Al 1100 alloy under different pre-heat treatment conditions.

2 Experimental

Al 1100 alloy sheet with composition of 99.0% Al, 0.42% Fe, 0.225% Si, 0.09% Cu, 0.32% Mn, 0.004% Zn and 0.011% Ga was purchased from Lian Giap & Co. Sdn. Bhd. The sheet is flat rolled and was cut into a dimension of 100 mm × 50 mm × 1.2 mm. At the beginning of the process, Al 1100 alloy underwent pre-heat treatment which was pre-annealing at 250 °C for 2 h and pre-solution treatment at 540 °C for 1 h followed by quenching in water. The sample was then rolled in a single stand rolling mill. The rolling was conducted up to a true strain of 0.70. Cryorolling was carried out by dipping the sample in liquid nitrogen for 30 min, and then followed by rolling. In between the rolling passes, the sample was dipped in liquid N_2 to maintain the cryogenic temperature.

Microstructural chacterization was performed using optical (model Meiji equipped with image analyzer i-Solution DT software) and high-resolution transmission electron microscope (HRTEM). High resolution TEM (model Technai F200) was performed at MIMOS Berhad. The edge of the sample that comprises the region of interest was polished and mounted. Then, the mounted sample was placed into the focus ion beam (FIB) model Helios Nanolab 650 and the region of interest was made parallel to the ion beam. A dual focused ion beam with a Ga ion source was used for the preparation of the TEM cross-section samples. D8 Bruker Advanced X-ray diffractometer was used to measure the crystallite size, lattice strain and dislocation density of the sample for 2θ ranging from 10° to 90°. Both XRD and HTREM samples were prepared from the CR sheets by randomly selecting the section along the direction of rolling. The Vickers hardness testing was conducted at room temperature with a load of 100 g and a dwell time of 10 s. For the tensile test, the specimens were machined into the ASTM E8 sub-sized specimen with a gauge length of 25 mm. A tensile test was conducted on an Instron universal testing machine at a crosshead speed of 1 mm/min until the samples failed.

The corrosion behaviour of the cryorolled Al 1100 alloys under different processing conditions was studied using potentiodynamic polarization of the specimens in simulated sea water solution. The instrument used was equipped with a working electrode, platinum counter electrode, and saturated calomel reference electrode connected to a potentiostat for the regulation of the potential and measurement of current. Potentials were scanned from −2.0 to +2.0 V at a scan rate of 0.005 V/s. The corrosion properties of the tested samples were characterized by the Tafel extrapolation method. Corrosion potential, corrosion current density, and corrosion rates from the polarization curves were measured. The electrolyte (artificial sea water) was prepared by mixing 3.5 wt.% sodium chloride (NaCl) in distilled water, using a magnetic stirrer. The samples were passivated in 3.5% NaCl solution, and the electrochemical test was stopped before the pitting potential was reached.

3 Results and discussion

3.1 Microstructural analysis

The optical micrographs of as-received material and cryorolled samples at different processing conditions are shown in Fig. 1. As presented in Figs. 1(b, c, d), the cryorolled (CR) samples exhibited severely deformed grains which were elongated along the rolling direction and were measured based on grain aspect ratio as tabulated in Table 1. The grain aspect ratio of the grain was estimated based on the ratio of grain length, *l*, to grain width, *w*. The value represents the distortion of grains as the deformation occurred [13,14]. From Table 1, it can be observed that initial heat treatment before cryorolling affected the value of the grain aspect ratio. The pre-annealed CR sample exhibited the highest grain aspect ratio, which indicated heavy deformed structure compared with other samples.

3.2 Structural analysis

The XRD patterns of as-received and cryorolled samples are shown in Fig. 2. A preferred orientation along (220) plane is observed in the rolled samples and this is due to the accumulation of rolling strain in rolling direction [15]. Meanwhile, peak broadening is due to the formation of refined grains (crystallite size) and enhanced micro-strain (lattice strain) [16]. Scherrer equation was used for calculating the lattice strain and crystallite size from the XRD data, and the dislocation density is obtained based on the equation reported by ANAS et al [17]. Table 2 tabulates the crystallite size, lattice strain and dislocation density values. There is a contrasting pattern in crystallite size and lattice strain for as-received and cryorolled samples. The crystallite size is decreased with increasing lattice strain. The as-received material has crystallite size

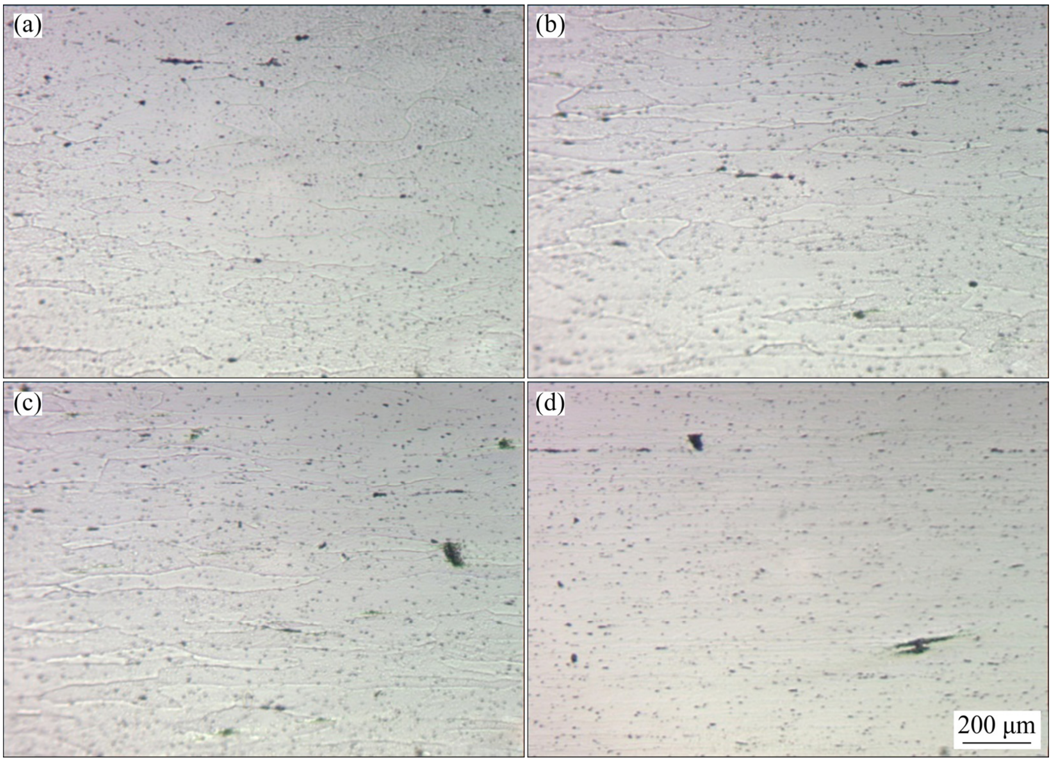

Fig. 1 Optical micrographs of as-received material (a), non pre-treated CR (b), pre-annealed CR (c) and pre-solution treated CR (d) samples

Table 1 Grain aspect ratios of as-received and cryorolled (CR) samples

Sample	Grain aspect ratio
As-received material	1.13
Non pre-treated CR	2.23
Pre-annealed CR	4.43
Pre-solution treated CR	4.23

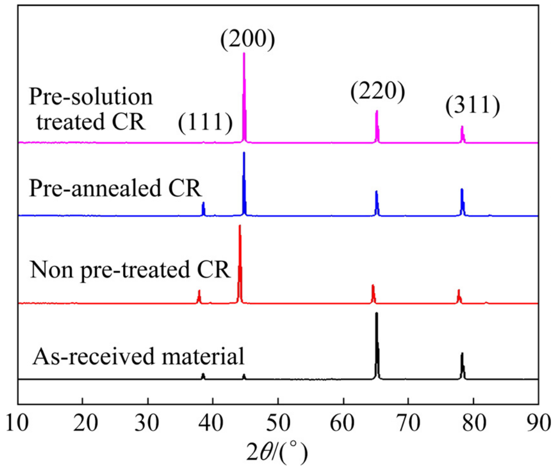

Fig. 2 XRD pattern of as-received and cryorolled Al 1100 alloy under various processing conditions

Table 2 Crystallite size, lattice strain and dislocation density of Al 1100 alloy under various processing conditions

Sample	Crystallite size/nm	Lattice strain/10^{-3}	Dislocation density/(10^{13} m^{-2})
As-received material	70.46	1.40	4.528
Non pre-treated CR	47.37	4.40	17.27
Pre-annealed CR	37.53	9.12	45.16
Pre-solution treated CR	46.53	8.90	35.50

of 70.46 nm. In the case of cryorolled samples without pre-treatment, the crystallite size is reduced by 32.8% (47.37 nm), and the lattice strain and dislocation density are increased by 214.3% (4.40×10^{-3}) and 281.4% (17.27×10^{13} m^{-2}) compared to those of as-received material.

However, for pre-treatment, the crystallite size of pre-annealed CR sample is reported to be 37.53 nm with lattice strain of 9.12×10^{-3} and dislocation density of 45.16×10^{13} m^{-2}. However, for pre-solution treatment, the crystallite size is observed to be 46.53 nm with lattice strain of 8.90×10^{-3} and dislocation density of 35.5×10^{13} m^{-2}. This study clarified that initial microstructure from pre-treatment affected the obtained value of the crystallite size, lattice strain and dislocation density. The realignment of dislocations during pre-annealing contributed to the ease of rolling at cryogenic temperature. As a result, high dislocation density is generated in pre-annealed sample and the anhilation of dislocation is suppressed [18]. The accumulation of dislocation density stores large amount of recrystallization power, producing UFG structures that require less strain [19,20]. In comparison, dislocations are stabilized in solution-treated samples. Thus, the dislocations are annihilated, leading to less dislocation density and difficulty in achieving UFG structure in subsequent CR treatment.

Variation in intensity is noted from the XRD patterns and the intensity of (220) plane is considerably decreased with deformation at various pre-treatments. As can be seen in Fig. 2, the intensity of (220) plane is less after cryorolling when compared to the other planes and this implies that the rotation of the grains in the plane (220) is preferable. This also suggests that the plane (220) is parallel with the surface rolled. Also, the stored energy in the rolled samples is also responsible for the preferred orientation [21].

3.3 HRTEM studies

Figure 3 presents high-resolution electron microscope (HRTEM) micrographs of pre-annealed (250 °C) CR samples. Highly deformed micro-structure with high density of dislocations in the form of dislocation cells and forests is observed. It has been well demonstrated that deformation at cryogenic temperature can suppress dynamic recovery and lead to a high dislocation volume in the structure due to the severe strain imposed into the material. The dislocations generated continually evolve into tangles/cell dislocations and sub-grain boundaries, finally forming new grain boundaries to develop new fine grains [22]. The restriction of dynamic recovery accumulates the dislocations that can be rearranged to form a sub-grain structure [23].

Two types of grains were observed in Fig. 3(a), equiaxed and elongated grain, as shown in red circles. The equiaxed grain size is in the range of 0.1−0.5 μm. The elongated grain has the length in

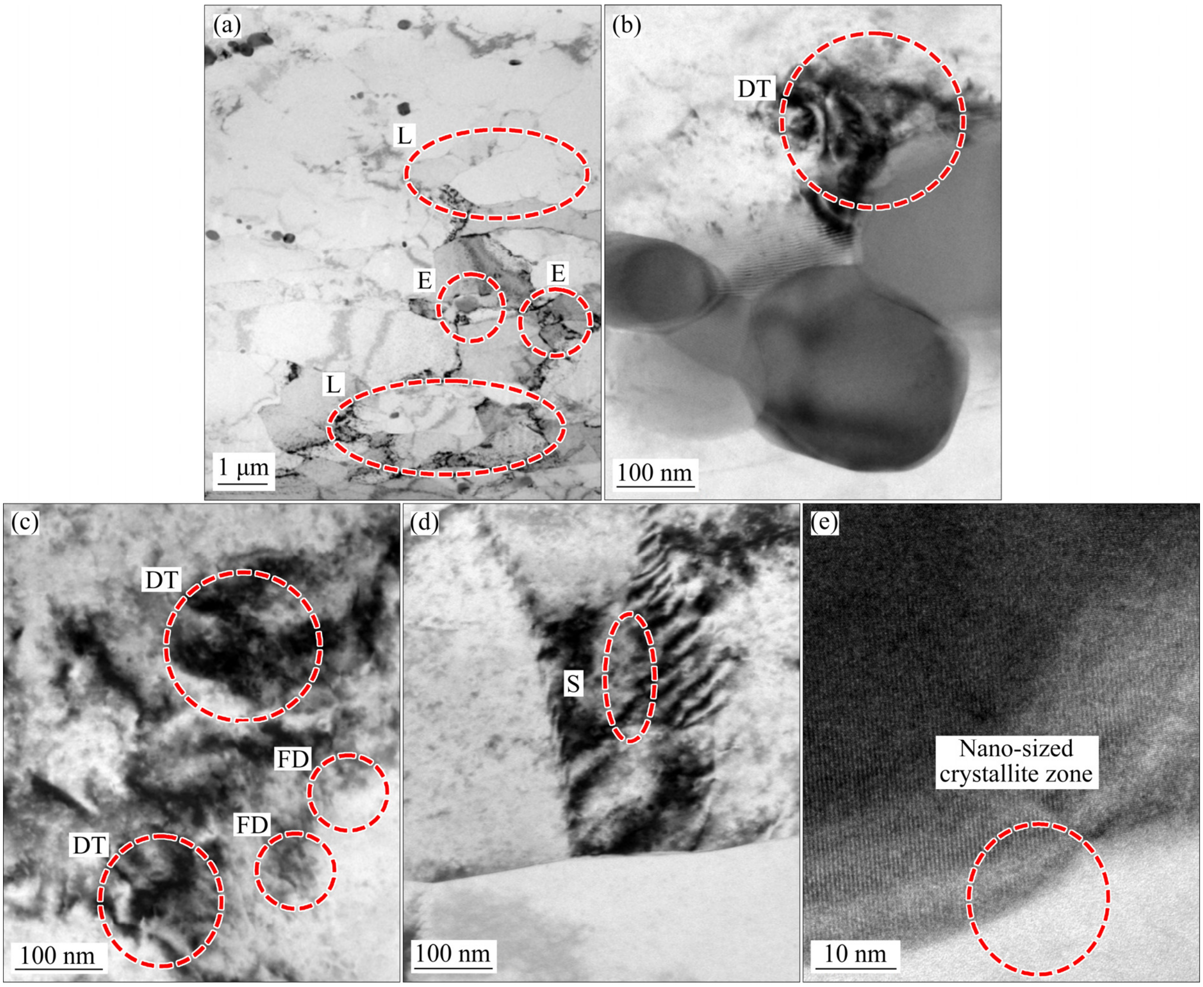

Fig. 3 HRTEM micrographs of pre-annealed CR sample showing fine sub grains and dislocation cells (L−Elongated grain; E−Equaixed grain; S−Submicron grain; DT−Dislocation tangle; FD−Fine dislocation)

the range of 1−4 μm and a width of 0.5 μm. Figure 3(b) shows that grain size is in nano metric scale. The deformed sub-grain structures (as shown in Fig. 3(d)) were visible in the TEM images. Numerous dislocation tangled zones with fine dislocation cells can be seen in Fig. 3(c). During rolling, a significant amount of strain energy is accumulated in the form of dislocations. Cross-slip occurs easily in Al alloys (with FCC structure) due to high stacking fault energy and dislocation sub-structures are found to be of a diffused type [24]. Ultrafine grained are produced by grain refinement in cryorolling process, as low rolling temperatures effectively inhibit the process of recovery [25]. Figure 4 shows the selected area electron diffraction pattern (SAED) reported from the central region of the micrograph shown in Fig. 3. As can be seen in Fig. 4, the corresponding ring pattern indicates that the deformed grain sub-structure is a low angle grain boundary.

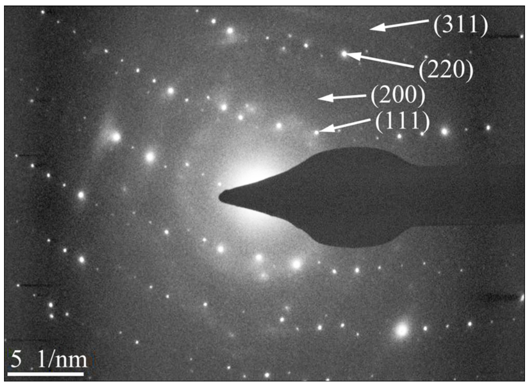

Fig. 4 SAED pattern taken from central region of image in Fig. 3

The HRTEM micrographs of the pre-solution treated CR samples are presented in Fig. 5. The bright-field TEM image with a low magnification in Fig. 5(a) shows equiaxed and elongated grains formed after the deformation process (as shown by the red circle in Fig. 5(a)). The pre-solution treated

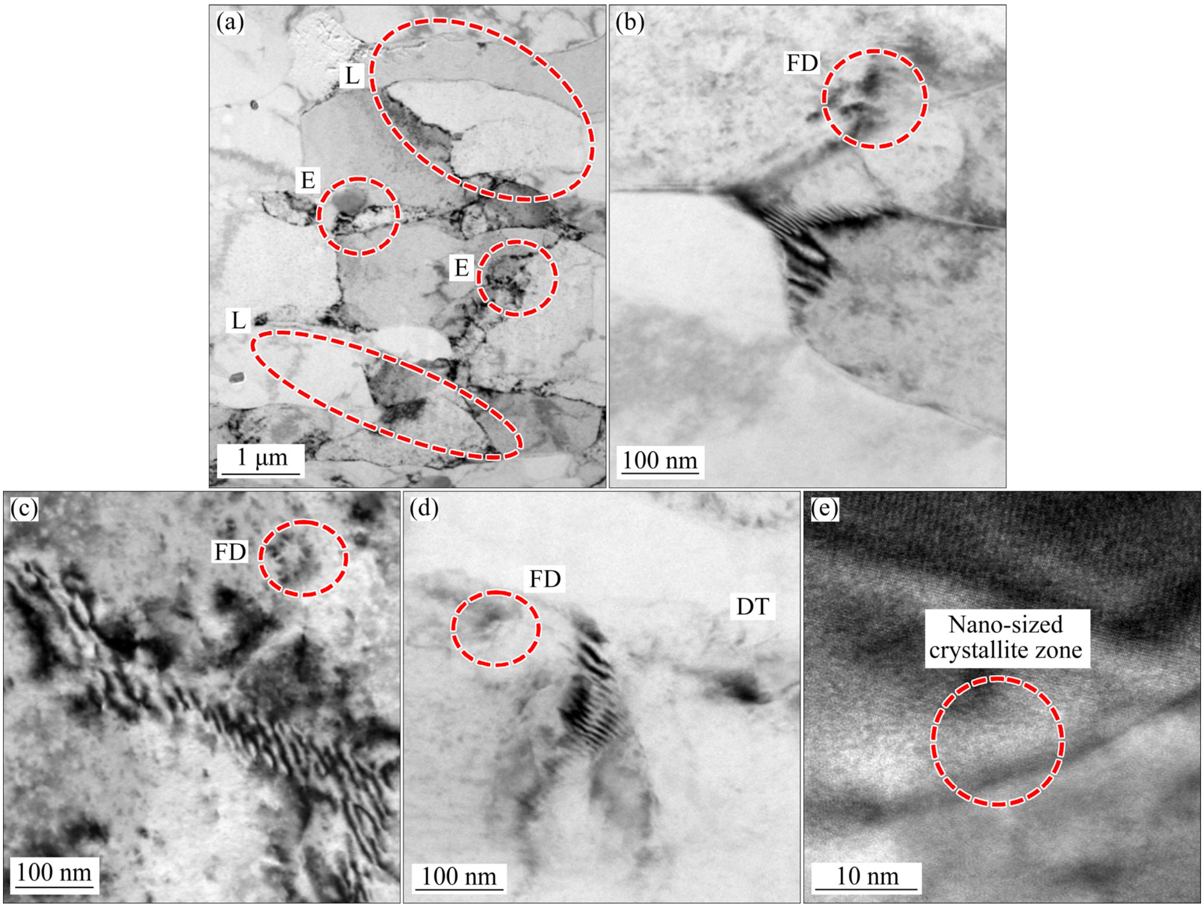

Fig. 5 HRTEM micrographs of pre-solution treated CR sample showing dislocation cell/substructures

CR sample exhibits the grain size within the range of 0.1−0.8 μm. Well-defined grain boundaries with highly deformed grains are also observed in Figs. 5(b, c). Figure 5(b) reveals the ultrafine-grained size of the nanoscale.

Deformed sub-grains can be observed in Figs. 5(c, d). The formation of subgrains in the CR sample is high due to the suppression of dislocation, which accumulates a large number of dislocations in the grain. The high density of dislocations tends to reach saturated value, and thus the dislocation begins to rearrange and forms a large number of subgrains [26]. The selected area electron diffraction pattern (SAED) is presented in Fig. 6. The corresponding ring pattern is not observed, but the average length between the bright spots can be determined. The SAED pattern indicates that the deformed grain has a low angle grain boundary. Pre-annealed CR sample has smaller grain size compared with the pre solution treated CR sample. This indicates that sample pre-annealed followed by cryrolling experiences high deformation with high dislocation density (45.16×10^{13} m^{-2}).

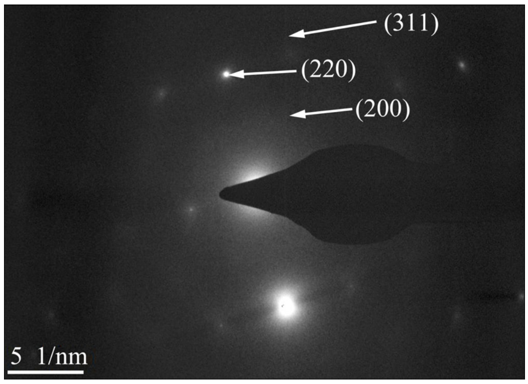

Fig. 6 SAED pattern taken from central region of image in Fig. 5

3.4 Hardness analysis

Figure 7 shows the effect of cryorolling on the hardness of Al 1100 alloy with the influence of initial heat treatment prior to cryo-rolling. The hardness value increased from 37.56 to 44.84 HV (by ~19%), 64.32 HV (by ~71%) and 52.43 HV (by ~40%) for non-pretreated CR, pre-annealed CR, and pre-solution treated CR samples, respectively. Increase in the hardness of the pre-annealed CR sample compared to the pre-solution treated CR sample is due to an improvement in dislocation density during cryorolling process. The increase in hardness is also due to grain refinement, and high dislocation density as observed by the TEM micrograph of pre-heat-treated CR sample [27].

In addition, the maximum hardness reported by the pre-annealed CR sample is due to the effective suppression of dynamic recovery. The pre-annealed CR sample has the highest increment in hardness values due to the removal of internal stresses and the formation of initial dislocation configuration which allow the material to deform more during cryorolling. The pre-solution treated CR sample exhibits comparatively lower hardness but higher dislocation density in some areas. Low level of alloying elements present in the alloy does not add significantly to the solid solution strengthening in solution treatment. However, on quenching after solution treatment, some favorable initial dislocation configuration may be obtained, resulting in high dislocation density in some areas on cryorolling as compared to the sample cryorolled without any pre-treatment.

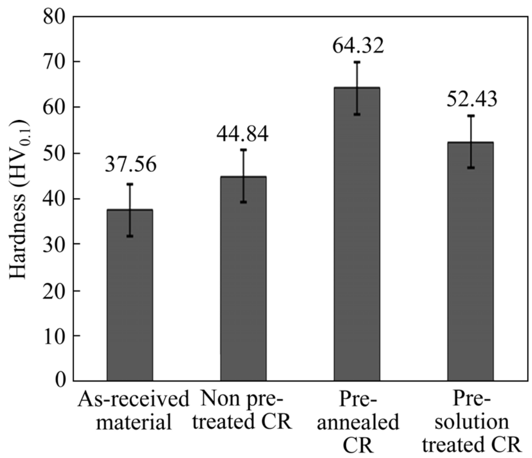

Fig. 7 Microhardness values of as-received material and cryorolled samples under various processing conditions

3.5 Tensile properties

Figure 8 presents the tensile properties of as-received material and cryorolled samples. Alloy subjected to different pre-heat treatments followed by cryorolling showed significant effect on ultimate tensile strength (UTS) and yield strength (YS). The UTS increased from 120.45 to 139.67 MPa (13% increment), and YS increased from 85.27 to 93.42 MPa (9% increment), while elongation decreased from 7.13 to 2.64 mm for non-pre treated CR samples. The UTS and YS increased from 120.45 to 174.10 MPa and from 85.27 to 112.41 MPa, respectively, in the pre-annealed CR sample. As for pre-solution treated CR sample, they increased to 141.42 and 98.68 MPa, respectively. The elongation for both samples decreased from 7.13 to 2.97 mm for the pre-annealed CR sample and 3.43 mm for the pre-solution treated CR sample. The high strength for CR sample is obtained due to the dislocation strengthening by heavy accumulation of dislocation in the material. Dynamic recovery is suppressed, leading to the dense dislocations in the microstructures of the material (evident from dislocation tangles and fine dislocation clusters in the TEM micrograph) [28]. In addition, strength of CR samples also increased because of the presence of submicrometric-sized UFG microstructure compared to the coarse-grained microstructure in the as-received material. These UFG materials have rhombic-shaped grains with high relative misorientation angles. They contain non-ordered dislocation tangles and clusters within the grains. These rhombic grains were formed due to the intersection of thin cell blocks orthogonally aligned to one another [29]. Also, additional dislocations are generated during the tensile testing of the CR sample, which interact quickly with the pre-existing fine dislocation clusters and tangles. More energy is then needed to remove the obstruction caused by the pre-existing dislocations, and the stress required to deform the material increases.

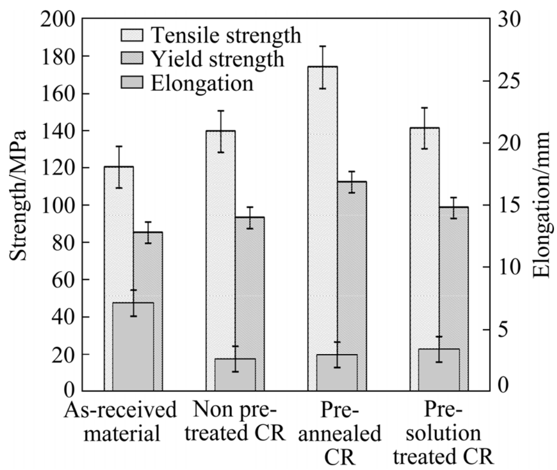

Fig. 8 Tensile properties of as-received material and cryorolled samples under various processing conditions

The tensile properties of Al 1100 alloy undergoing pre-annealing treatment followed by cryorolling process were found to be superior to those of non-pretreated CR and pre-solution treated CR samples. Pre-annealing prior to cryorolling results in conducive microstructural changes. The removal of internal stresses and residual dislocations results in better mechanical properties of the deformed alloy [30]. The suppression of recovery and cross-slip during cryorolling leads to the formation of more defects (dislocations) which will serve as sites for grain nucleation. As a result, ultrafine grains are formed, resulting in increased strength [31]. In addition, the improvement in the strength for pre-annealed CR sample is found to be more in comparison with the pre-solution treated CR sample due to the grain boundary strengthening resulted from evolution of UFG microstructure as noticed from TEM micrographs (Figs. 3(a−f)).

3.6 Fracture analysis

Fracture surface after tensile testing was observed on SEM to understand the mechanism of failure for different pre-heat treated samples. Fractured surface morphologies of samples under various processing conditions are shown in Fig. 9. All the samples were fractured in a ductile and brittle manner. The tensile fracture surface consists of well-developed dimples on the surface and rough and deep craters inside the samples. Dimpled rupture is characterized by equiaxed dimples formed on the fracture surface due to the coalescence of micro voids. Fractographs of the as-received sample reveal the presence of several coarse dimples with size varying from 5 to 20 μm (Fig. 9(a)). The grain boundaries are the weak link in the microstructure, serving as the starting point for fractures in the material. The coarse dimples corroborate well with the large ductility of as-received samples.

The CR sample shows the appearance of mixture of coarse and fine dimples. The dimples in CR sample are sharp and slightly elongated in the shear direction (Figs. 9(b−d)). This strongly points to shear-dominated fracture mechanism. Shear-dominated fractures are typical in heavily cold-worked materials due to an elevated rate of plastic

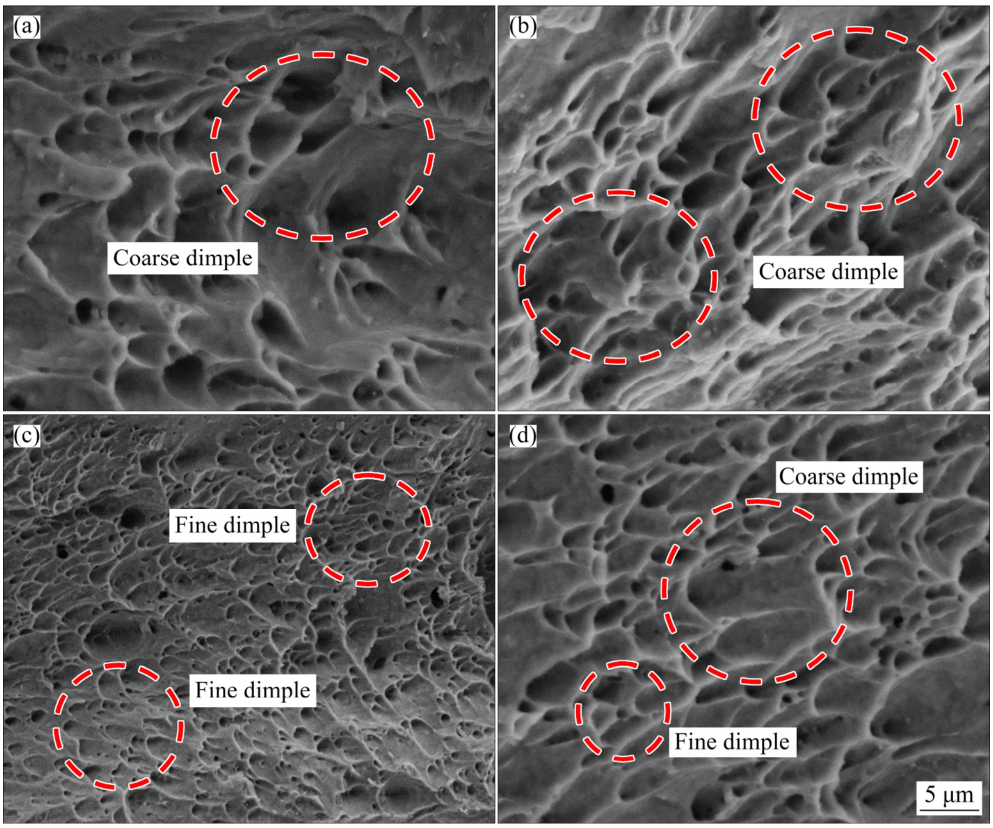

Fig. 9 Fractured surface morphologies of as-received material (a), non pre-treated CR (b), pre-annealed CR (c) and pre-solution treated CR (d) samples

instability. This causes the material to be sheared and separated, leaving behind a trail of elongated and shallow dimples [29]. The cryorolled pre-annealed samples have the finest dimple size with an average size of 3 μm dispersed throughout the fracture surface. In the pre-annealed CR sample, the grain refinement encourages various nucleation sites which further coalesce and prevent the micro voids from growing to a larger size. This might be the possible reason for the reduction in dimples size with increasing grain refinement. KRISHNA et al [32] reported that the decrease in dimple size was caused by a large amount of deformation energy and work hardening that occurred during severe plastic deformation.

3.7 Corrosion analysis

Pre-heat treatment prior to cryorolling results in the changes in microstructure, dislocation density and configuration. The polarization curves of as-received material and cryorolled samples with different initial heat treatments were compared (Fig. 10). The result shows that the polarization curve of as-received material shifts to more negative φ_{corr} (−1.1605 V) and it has the highest I_{corr} (5.49 μA) value with the corrosion rate of 0.1722 mm/year. However, the corrosion rate of as-received material dropped to 0.0786 mm/year after undergoing the cryorolling process (Table 3).

A better corrosion resistance was recorded as the sample underwent pre-annealing and solution treatment with the value of φ_{corr} (−1.0291 and −1.0281 V), and I_{corr} (1.66 and 2.9 μA), and

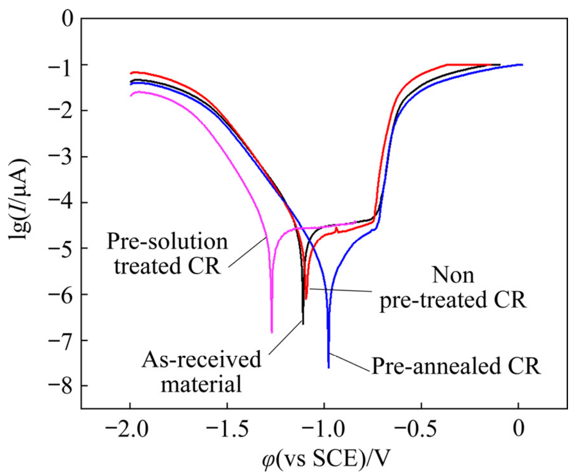

Fig. 10 Potentiodynamic polarization curves of as-received and cryorolled samples under various processing conditions

Table 3 Electrochemical data for as-received material and cryorolled samples

Sample	φ_{corr}(vs SCE)/V	I_{corr}/μA	Corrosion rate/(mm·year^{-1})
As-received material	−1.1605	5.49	0.1722
Non pre-treated CR	−1.0916	4.77	0.0786
Pre-annealed CR	−1.0291	1.66	0.0352
Pre-solution treated CR	−1.0281	2.9	0.0354

corrosion rates are 0.0352 and 0.0354 mm/year, respectively. The high corrosion resistance is related to the number of grains formed in the material. As the number of grains is large, the average grain boundary area would be high, causing more chloride ions to react with the surface of the aluminium alloy. The decrease in I_{corr} value led to a reduction in the concentration of chloride per grain boundary, resulting in a decrease in the material corrosion rate [33]. RALSTON and BIRBILIS [34] reported similar findings which claimed that the better corrosion resistance (with corrosion current density of 1.5−2.0 μA/cm^2) of the sample was correlated with different sizes from 100 μm to 20 nm of grains produced during plastic deformation.

High corrosion resistance of an alloy can be explained by the amount of oxide layer formed during the passivation process, as presented in Fig. 11. The fine structure has a large area of grain boundary, creating a high number of active sites for rapid formation of continuous and protective passive film. As a result, the formation of high density nucleation sites for passive films leads to high fraction of passive layers and low corrosion rates [35]. According to SONG et al [36], the passive films are prone to nucleate at the crystalline defects, such as grain boundaries and dislocations. The cryorolled sample has a lot of crystalline defects with high internal energy, such as dislocation and large fractions of high angle and low angle grain boundaries. Those energetic crystalline defects provide more stored energy for the growth of the passive film. The passive film acts as a physical barrier to corrosion or further oxidation process. When the UFG sample is immersed in aqueous solution, a more rapid growth of the passive film will occur, which will grow to a thicker value than that on the as-received material.

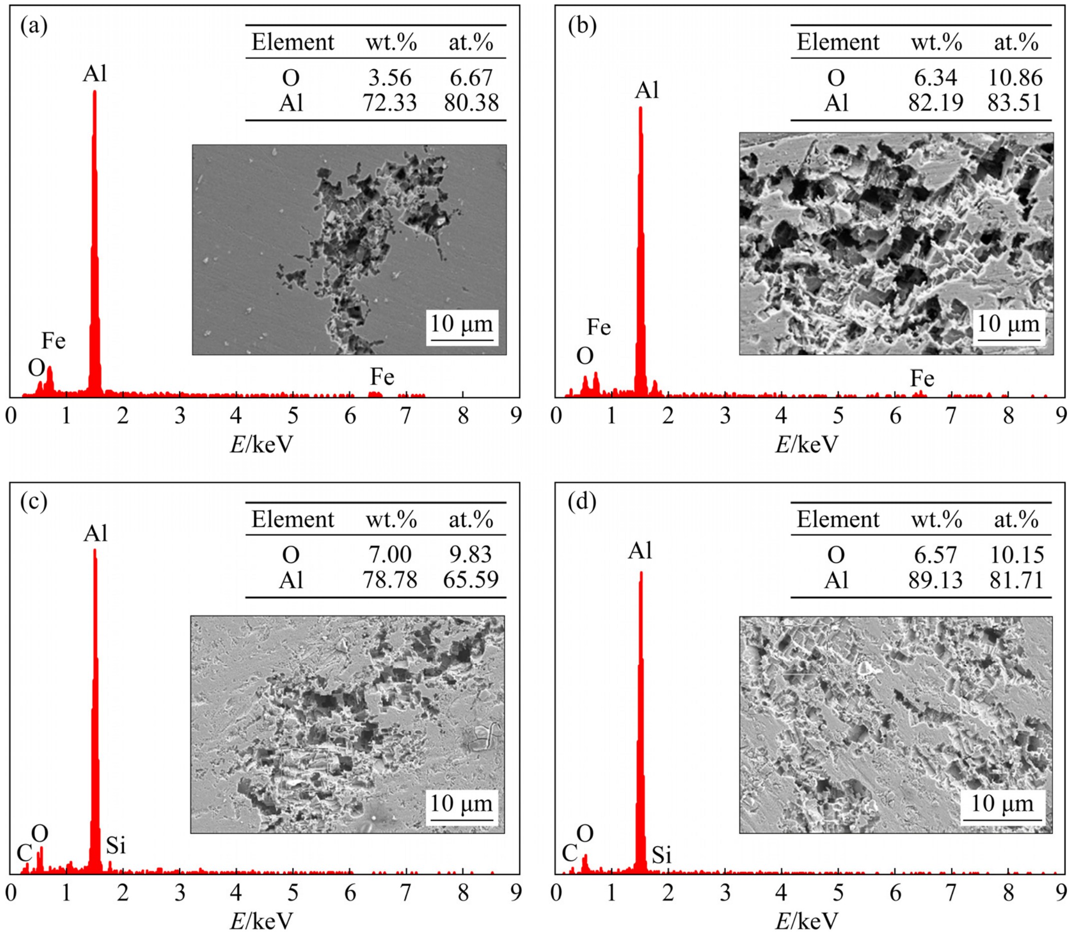

Fig. 11 Morphology and constitution of oxide layer formed on as-received material (a), non pre-treated CR (b), pre-annealed CR (c) and pre-solution treated CR (d) samples

The pre-annealed CR sample shows the highest content of oxygen (7 wt.%) compared to other samples (Table 4). The high oxygen content of the pre-annealed CR sample may be related to the presence of the passive layer on the surface of the sample. The highly passive layer was due to the distribution of grains during the deformation process. As corrosion occurred, the presence of Cl^- ions attacked the crystalline lattice defects such as grain boundary and dislocation, resulting in the formation of an oxide layer. The high number of grain boundary and the dislocation density formed after undergoing heat treatment and cryorolling process resulted in improved corrosion properties. The large number of grain boundaries have higher energy than the bulk of the material, which enhances electron diffusion and leads to a more stable passive film and, therefore enhanced corrosion resistance [37].

Table 4 Contents of oxide layer formed on as- received and cryorolled samples

Sample	Content of oxide film/wt.%
As-received material	3.56
Non pre-treated CR	6.34
Pre-annealed CR	7.00
Pre-solution treated CR	6.57

The strength of the pre-solution treated CR sample did not show significant improvement compared to non pre-heat treated CR sample due to very little difference in the grain refinement. However, much improved corrosion properties for the pre-solution treated CR sample as compared to the non pre-heat treated CR sample may be due to the better dislocation configuration in the pre-solution treated sample that also seems to relate to the corrosion behavior.

4 Conclusions

(1) Effect of pre-heat treatment on cryorolling of Al 1100 alloy was characterized from micron scale to nano scale structure development. Cryorolling in general and pre-heat treatment followed by cryorolling in particular resulted in high dislocation density, grain refinement and large strains, which are major contributing factors in enhancing mechanical properties (strength and hardness) as compared to as-received condition. X-ray diffraction and HRTEM studies bring out the above features distinctively in the variously treated samples.

(2) The significant improvement in strength (UTS of 174.10 MPa, YS of 112.41 MPa, and elongation of 2.97 mm) is observed in the samples obtained through the pre-annealed CR compared to pre-solution treated CR samples (UTS of 141.42 MPa, YS of 98.68 MPa, and elongation of 3.43 mm). The increase in strength is attributed to the accumulation of dislocation density and ultrafine grains. The pre-annealed sample exhibited the highest grain aspect ratio (4.43), the smallest crystallite size (37.53 nm), the highest lattice strain (9.12×10^{-3}) and the highest dislocation density (45.16×10^{13} m^{-2}).

(3) Better corrosion resistance was recorded for samples undergoing pre-treatment. Pre-annealed CR sample has the best corrosion resistance. This is due to the high number of grains, which increases the total area of grain boundaries and hence results in the formation of large passive layers. Pre-solution treated samples perhaps provided dislocation sites, resulting in more passivation and thus improved corrosion resistance.

Acknowledgments

The authors would like to thank to Universiti Sains Malaysia for providing the fund for this study under RU grant No. 1001/PBahan/8014105.

References

[1] ZAKARIA S A, HUSSAIN Z, SEMAN A A. Effects of cold rolled and cryorolled on microstructures and mechanical properties of aluminium 1100 alloy [C]//Proc AIP Conference 2068. Materials Characterization using X-rays and Related Techniques. New York: AIP Publishing, 2019: 1−6. https://doi.org/10.1063/1.5089385.

[2] KRYMSKIY S, SITDIKOV O, AVTOKRATOVA E, MARKUSHEV M. 2024 aluminum alloy ultrahigh-strength sheet due to two-level nanostructuring under cryorolling and heat treatment [J]. Transactions of Nonferrous Metals Society of China, 2020, 30: 14−26.

[3] MEI L, CHEN X P, HUANG G J, LIU Q. Improvement of mechanical properties of a cryorolled Al−Mg−Si alloy through warm rolling and aging [J]. Alloys and Compounds, 2019, 777: 259−263.

[4] ZHANG Peng-chao, SHI Jie-fu, YU Ying-shui, SUN Jun-cai, LI Ting-ju. Effect of cryorolling on microstructure and property of high strength and high conductivity Cu−0.5wt.%Cr alloy [J]. Transactions of Nonferrous Metals Society of China, 2020, 30: 2472−2479.

[5] WANG Y M, CHEN M W, ZHOU F H, MA E. High tensile ductility in a nanostructured metal [J]. Nature, 2002, 419: 912−915.

[6] FULORIA D, GOEL S, JAYAGANTHAN R, SRIVASTAVA D, DEY G K, SAIBABA N. Mechanical properties and microstructural evolution of ultrafine grained zircaloy-4 processed through multiaxial forging at cryogenic temperature [J]. Transactions of Nonferrous Metals Society of China, 2015, 25: 2221−2229.

[7] RAO P N, SINGH D, JAYAGANTHAN R. Effect of annealing on microstructure and mechanical properties of Al 6061 alloy processed by cryorolling [J]. Journal of Materials Science and Technology, 2013, 29: 76−82.

[8] KRISHNA K G, SINGH K N, VENKATESWARLU K C, HARI KUMAR K C. Tensile behavior of ultrafine-grained Al−4Zn−2Mg alloy produced by cryorolling [J]. Materials Engineering and Performance, 2011, 20: 1569−1574.

[9] PANIGRAHI S K, JAYAGANTHAN R. Development of ultrafine-grained Al6063 alloy by cryorolling with the optimized initial heat treatment [J]. Material and Design, 2011, 32: 2172−2180.

[10] SEKHAR K C, NARAYANASAMY R, VELMANIRAJAN K. Experimental investigations on microstructure and formability of cryorolled AA 5052 sheets [J]. Material and Design, 2014, 53: 1064−1070.

[11] GASHTI S O, FATTAH-ALHOSSEINI A, MAZAHERI Y, KESHAVARS M K. Effects of grain size and dislocation density on strain hardening behaviour of ultrafine grained A1050 processed by accumulative roll bonding [J]. Journal of Alloys and Compounds, 2016, 658: 854−861.

[12] SIVAPRASAD K, SWARNALATHA V, RAVIKUMAR V V, MUTHUPANDI V. Influence of short annealing treatment on corrosion behaviour of cryorolled commercially pure aluminium [J]. Anti-Corrosion Methods and Materials, 2010, 57: 18−20.

[13] AHMAD E, KARIM F, SAEED K, MANZOOR T, ZAHID G H. Effect of cold rolling and annealing on the grain refinement [J]. IOP Conference Series: Materials Science and

Engineering, 2014, 60: 1−8. doi: 10.1088/1757-899X/60/1/012029.

[14] SINGH D, NAGESWARA RAO P, JAYAGANTHAN R. Microstructures and impact toughness behavior of Al 5083 alloy processed by cryorolling and afterwards annealing [J]. International Journal of Minerals, Metallurgy and Materials, 2013, 20: 759−769.

[15] KRISHNA K S V B R, CHANDRA K S, TEJAS R, NAGA N K, SIVAPRASAD K, NARAYANASAMY R, VENKATESWARLU K. Effect of cryorolling on the mechanical properties of AA5083 alloy and the Portevin-Le Chatelier phenomenon [J]. Materials and Design, 2015, 67: 107−117.

[16] UNGAR T. Microstructural parameters from X-ray diffraction peak broadening [J]. Scripta Materialia, 2004, 51: 777−781.

[17] ANAS N M, ABIOYE T E, ANASYIDA A S, DHINDAW B K, ZUHAILAWATI H, AZZURA I. Microstructure, mechanical and corrosion properties of cryorolled-AA5052 at various solution treatment temperatures [J]. Materials Research Express, 2020, 7: 016535.

[18] SINGH D, NAGESWARA R P, JAYAGANTHAN R. Effect of deformation temperature on mechanical properties of ultrafine grained Al−Mg alloys processed by cryorolling [J]. Materials and Design, 2012, 50: 646−655.

[19] LI Chang, XIONG Han-qing, BHATTA L, WANG Lin, ZHANG Zhao-yang, WANG Hui, KONG C, YU Hai-liang. Microstructure evolution and mechanical properties of Al−3.6Cu−1Li alloy via cryorolling and aging [J]. Transactions of Nonferrous Metal Society of China, 2020, 30: 2904−2914.

[20] QUAN Guo-zheng, ZHANG Yu-qing, ZHANG Pu, MA Yao-yao, WANG Wei-yong. Correspondence between low-energy twin boundary density and thermal-plastic deformation parameters in nickel-based superalloy [J]. Transactions of Nonferrous Metals Society of China, 2021, 31: 438−455.

[21] VIGNESHWARAN S, SIVAPRASAD K, NARAYANASAMY R, VENKATESWARLU K. Microstructure and mechanical properties of Al−3Mg−0.25Sc alloy sheets produced by cryorolling [J]. Materials Science and Engineering A, 2019, 740−741: 49−62.

[22] SONG D, WANG Guo-wei, ZHOU Z, KLU E E, GAO B, MA A, WU Y, SUN Jia-peng, JIANG Jing-hua, MA Xiao-long. Developing a high-strength Al−11Si alloy with improved ductility by combining ECAP and cryorolling [J]. Materials Science and Engineering A, 2020, 773: 138880.

[23] ABBASI M B, KARIMZADEH F, ENAYATI M H. Mechanical and tribological behavior of severely plastic deformed Al6061 at cryogenic temperatures [J]. Materials Science and Engineering A, 2017, 683: 56−63.

[24] KRISHNA K S V B R, ASHFAQ M, VARUN V, SIVAPRASAD K, VENKATESWARLU K, AKELLA S S R. On plastic deformation behavior of cryorolled AA8090 alloy [J]. Transactions of the Indian Institute of Metals, 2017, 70: 1463−1475.

[25] JAYAGANTHAN R, BROKMEIER H G, SCHWEBKE B, PANIGRAHI S K. Microstructure and texture evolution in cryorolled Al 7075 alloy [J]. Alloy and Compounds, 2010, 496: 183−188.

[26] KUMAR N, JAYAGANTHAN R, BROKMEIER H G. Effect of deformation temperature on precipitation, microstructural evolution, mechanical and corrosion behavior of 6082 Al alloy [J]. Transactions of Nonferrous Metals Society of China, 2017, 27: 475−492.

[27] MAGALHAES D C C, KLIAUGA A M, FERRANTE M, SORDI V L. Plastic deformation of FCC alloys at cryogenic temperature: The effect of stacking-fault energy on microstructure and tensile behavior [J]. Materials Science, 2017, 52: 7466−7478.

[28] ABASSI-BAHARANCHI M, KARIMZADEH F, ENAYATI M H. Thermal stability evaluation of nanostructured Al6061 alloy produced by cryorolling [J]. Transaction of Nonferrous Metals Society of China, 2017, 27: 754−762.

[29] DHAL A, PANIGRAHI S K, SHUNMUGAM M S. Deformation behaviour and fracture mechanism of ultrafine-grained aluminium developed by cryorolling [C]//Strengthening and Joining by Plastic Deformation. Spinger Nature Singapore Pte Ltd, 2019: 31−52.

[30] JIANG Q W, LI X W. Effect of pre-annealing treatment on the compressive deformation and damage behaviour of ultrafine-grained copper [J]. Materials Science and Engineering A, 2012, 546: 59−67.

[31] BLESSTO B, SIVAPRASAD K, MUTHUPANDI V, SENTHIL P, ARUMUGAM M. Analysis of heat treatment response for cryorolled AA2219 alloy [J]. Transactions of the Indian Institute of Metals, 2019, 72: 1881−1900.

[32] KRISHNA N N, ASHFAQ M, SUSILA P, SIVAPRASAD K, VENKATESWARLU K. Mechanical anisotropy and microstructural changes during cryorolling of Al−Mg−Si alloy [J]. Materials Characterization, 2015, 107: 302−308.

[33] KRISHNA K G, SIVAPRASAD K, SANKARA NARAYAN T S N, HARI KUMAR K C. Localized corrosion of an ultrafine grained Al−4Zn−2Mg alloy produced by cryorolling [J]. Corrosion Science, 2012, 60: 82−89.

[34] RALSTON K D, BIRBILIS N. Effect of grain size on corrosion: A review [J]. Corrosion, 2020, 66: 1−13.

[35] BALYNOV A, KUTNYAKOVA J, AMIRKHANOVA N A, STOLYYAROV V V, VALIEV R Z, LIAO X Z, ZHAO Y H, JIANG Y B, XU H F, LOWE T C, ZHU Y T. Corrosion resistance of ultra-fine-grained Ti [J]. Scripta Materialia, 2004, 51: 225−229.

[36] SONG D, MA A B, JIANG J H, LIN P H, SHI J. Improving corrosion resistance of pure Al through ECAP [J]. Corrosion Engineering, Science and Technology, 2011, 46: 505−512.

[37] KORCHEF A, KAHOUL A. Corrosion behavior of commercial aluminum alloy processed by equal channel angular pressing [J]. International Journal of Corrosion, 2013: 983261. https://doi.org/10.1155/2013/983261.

退火和固溶处理对深冷轧 1100 铝合金力学性能和腐蚀性能的影响

S. A. ZAKARIA[1], A. S. ANASYIDA[1], H. ZUHAILAWATI[1], B. K. DHINDAW[2], N. A. JABIT[1], A. ISMAIL[3]

1. Structural Materials Niche Area, School of Materials & Mineral Resources Engineering, Universiti Sains Malaysia, 14300 Nibong Tebal, Penang, Malaysia;
2. Indian Institute of Technology Kharagpur 721302, India;
3. Department of Materials Engineering and Design Faculty of Mechanical and Manufacturing Engineering, Universiti Tun Hussein Onn Malaysia, 86400 Batu Pahat, Johor, Malaysia

摘　要：详细研究冷轧前退火和固溶处理对 1100 铝合金初始组织的形成、纳米至微米级组织的形成以及力学性能和腐蚀性能的影响。在 50%深冷轧前，先对样品在 250 °C 下预退火 2 h，或在 540 °C 下预固溶处理 1 h。利用 X 射线衍射和高分辨率透射电子显微镜技术研究加工后合金的晶粒尺寸、晶格应变和位错组态。结果表明，与预固溶处理的样品相比，预退火处理的样品具有最大的晶粒长宽比(4.43)、最小的晶粒尺寸(37.53 nm)、最高的晶格应变(9.12×10^{-3}) 和最高的位错密度(45.16×10^{13} m^{-2})。预退火样品的硬度、极限抗拉强度和屈服强度分别提高 43.44%、24.64%和 20.33%。与未经预处理的深冷轧样品相比，预退火和预固溶处理样品的耐腐蚀性更好，其中预退火样品的耐腐蚀性最好。

关键词：深冷轧制；1100 铝合金；预热处理；纳米组织；超细晶；力学性能；耐腐蚀性能

(Edited by Bing YANG)